Moisture Modeling: Effective Moisture Penetration Depth Versus Effective Capacitance

Jason Woods, PhD

Jon Winkler, PhD
Associate Member ASHRAE

Dane Christensen, PhD
Member ASHRAE

ABSTRACT

This paper compares two moisture models in the context of residential whole-building simulations—the effective moisture penetration depth (EMPD) model and the effective capacitance (EC) model. Previous research has shown that the EMPD model provides a more physically realistic response to humidity-load fluctuations than the EC model. But it is unclear how the choice of moisture model affects overall conclusions informing building design and equipment selection. In this study, the models are evaluated based on their ability to predict relative humidity, predict energy use, and to select HVAC equipment. Whole building simulations indicate that the EC and EMPD models are not equivalent, and that combining the capacitance of the building materials with the indoor air capacitance in the EC model is the root cause of this discrepancy. It means that the EC model cannot dampen humidity loads of different frequencies. This study also showed that a simulation using a certain value of EC in one city can agree with the EMPD results, but that the same EC value in a different city may not agree with the EMPD results. However, the results showed that some conclusions drawn from simulations using the EMPD model and the EC model may often be the same, even if the results differ.

INTRODUCTION

Humidity in residential buildings can cause problems, particularly in hot-humid climates. High relative humidity (RH) is associated with occupant discomfort (Fang et al. 1998), may lead to occupant health problems (Haverinen et al. 2003, Bornehag et al. 2004), and can damage building materials (Steeman, 2009). High efficiency constructions, such as high-insulation envelopes, can amplify these problems by reducing air-conditioner runtime (Rudd and Henderson 2007). Mechanical ventilation, as mandated by ASHRAE 62.2 (ASHRAE 2004), can also worsen the problem in hot-humid climates by introducing humid ventilation air (Walker and Sherman 2007). Several studies have since supported these findings, which show extensive periods of high indoor RH, which are possibly worse in high-performance, low energy homes (Henderson et al. 2008; Lstiburek 2009a; Lstiburek 2009b; Winkler et al. 2013).

Questions still remain on how to best control indoor RH. Modeling the transport and storage of moisture in buildings materials is important in answering these questions. Simulations tools such as WUFI (Künzel et al. 2001) can be used to predict and better understand moisture transport and storage inside wall assemblies. WUFI uses a finite-difference approach to solve for the profiles of temperature and moisture content inside the materials (Künzel 1995, Antretter et al. 2011). While useful when analyzing a wall assembly in detail, finite-difference methods take a long time to solve. In whole-building simulations, moisture modeling is often used to quickly analyze many design features for optimization purposes, as done by Winkler et al. (2013). Thus, this study is looking for alternatives to the finite-difference approach that achieve similar accuracy with a shorter runtime.

Current standard practice in whole-building energy simulations is to use an effective capacitance (EC) multiplier to account for the moisture buffering of partition walls, flooring, and furnishings (EPA 2001). While this EC multiplier is an

Jason Woods, Jon Winkler, *and* ***Dane Christensen*** *are research engineers in the Electricity, Resources, and Building Systems Integration Center at the National Renewable Energy Laboratory, Golden, CO.*

Published by ASHRAE 2013

improvement over neglecting the materials, it does not correctly model the transfer of moisture between the room air and the materials, since the materials and the room are combined into a single node. But it can be solved several orders of magnitude more quickly than the finite-difference approach.

Another approach is the effective moisture penetration depth (EMPD) model (Cunningham 1988; Kerestecioglu et al. 1990; Cunningham 1992), which has similar computation requirements as the effective capacitance approach, but is more physically realistic. A previous study compared the EMPD and EC models against an analytical solution for a simple test case and with a more advanced finite-difference model for two more complicated test cases. In each test case, Woods et al. (2013) found that a modified EMPD model (referred to there as $EMPD_2$) obtained closer results than the EC model.

Several researchers have looked at this moisture buffering effect with finite-difference modeling (Künzel et al. 2005; Rode and Grau 2008; Steeman et al. 2010; Tariku et al. 2011), EMPD modeling (Abadie and Mendonça 2009; Janssen and Roels 2009), or with tests on individual materials (Plagge et al. 2007; James et al. 2010). While some studies made simple comparisons between the EMPD and EC models (e.g., EPA 2001), it is unclear how their differences affect the overall conclusions from whole-building simulations. This is the focus of this study.

While there are other moisture-buffering related factors needed to ensure a simulation accurately represents a real building (e.g., moisture properties of materials), a physically accurate moisture model is a key factor. The purpose of this paper is to compare the EMPD and EC models for use in whole-building simulations. This paper describes the fundamental differences between these two models and compares their results to illustrate their ability to:

1. predict the indoor RH
2. estimate the energy use of temperature and humidity control
3. select appropriate air-conditioning and dehumidification equipment for a particular building

METHODS

The EC and EMPD models differ in the way they solve for moisture transfer into and out of walls and furnishings. This study explores the implications of these differences by using EnergyPlus, a whole-building energy simulation software (DOE 2012).

For this comparison, we simulate a 223 m^2 (2400 ft^2) house in two hot-humid cities: Houston and Orlando. These cities represent two major population centers in the Building America hot-humid climate zone (PNNL 2010), but provide some geographical variation. We use the same construction details as a recent study (Winkler et al. 2013), which is a home that represents 50% source energy savings over 2009 International Energy Conservation Code (IECC) requirements (ICC 2009). Key characteristics of this home are shown in Table 1. Internal gains from equipment, occupants, and domestic hot water use were simulated according to the Building America Housing Simulation Protocols (Hendron and Engebrecht 2010). The sensible gains varied based on the time of year and day of the week from 16.6–21.8 kWh/day, and latent gains varied from 3.4–3.7 kWh/day (4.95–5.3 kg of water per day or 10.9–11.7 lbs/day).

As mentioned in the Introduction, the simulations are used to compare how these models predict indoor RH, predict energy use, and select HVAC equipment. Specifically, this study investigates the following.

- **Indoor RH.** For predicting the indoor RH, we perform annual simulations without controlling humidity. We compare the RH profiles throughout the simulation period, and also look at the aggregate results that are often used to assess thermal comfort and the risk of mold growth (e.g., hours above 60% rh).
- **Energy Use.** We compare the energy use for cases without and with humidity control. The latter includes a 45 pints/day (21.3 L/day) dehumidifier to maintain the RH setpoint, with both 60% and 55% used for this setpoint. We also simulate a case with no moisture buffering for a baseline comparison.
- **HVAC Equipment Selection.** There are different strategies for controlling the RH in a building. Winkler et al. (2013) used the EMPD model to look at several equipment options for high-performance homes in hot-humid climates. We look at a few of the same equipment options to determine how those findings compare to the more commonly-used EC model. In addition to the baseline equipment in Table 1, we also simulate dehumidifiers of different sizes and a high efficiency, variable-speed air conditioner.

Table 1. Characteristics of High-Performance Home

Characteristic	Description
Foundation	Slab-on-grade, uninsulated
Walls	R-13, 2 × 4 16 in. on center + 1 in. of foam
Windows	U-Factor = 2.1 W/m^2·K (0.368 Btu/h·ft^2·°F); SHGC[a] = 0.3
Attic	Vented, R-30 blown-in fiberglass
Infiltration	0.00018 specific leakage area (3.7 air changes/h at 50 Pa)
Ventilation	Continuous, at ASHRAE Standard 62.2 rates 92 m^3/h (54 cfm)
HVAC	SEER 21 air conditioner, 78% AFUE[b] gas furnace, XX L/kWh dehumidifier (when used)
Ducts	Within conditioned space
Water heater	Gas tankless, (0.82 Energy Factor)
Appliances	ENERGY STAR®
PV	kW on unshaded rooftop

[a] SHGC = solar heat gain coefficient
[b] AFUE = annual fuel utilization efficiency

We run each of these simulations for both the EMPD and EC models. We perform two-year simulations and discard the results from the first year to eliminate any effects from the initial conditions. The EC model simulations were run in EnergyPlus v7.1, while the EMPD simulations were run using a custom version of EnergyPlus that includes a modified EMPD model (referred to as $EMPD_2$ in Woods et al. [2013]). The EC and EMPD models are described below.

Effective Capacitance (EC) Model

The fundamentals of the EC model are depicted in Figure 1a, which shows how a single node is used to represent the capacitance of the room air and its materials leading to the following equation:

$$\rho_{air}V(\mathrm{EC})\frac{d\omega_{room}}{dt} = \sum_{i=1}^{N}\dot{m}_{v,\,i} \tag{1}$$

On the left hand side, ρ_{air} is the density of air, V the volume of the room, ω_{room} the room air humidity ratio, and t time. The moisture capacitance of both the room air and the materials are lumped together with the effective capacitance, EC. For example, if EC = 20, the capacitance of the building materials is assumed to be 19 times larger than that of the air alone (1 unit from air + 19 units from materials = 20 units). It also assumed that the moisture content of the materials changes instantaneously with the room humidity, neglecting the finite mass transfer resistance between the room air and the materials. This last assumption is one of the key differences with the EMPD model described below.

The right hand side of Equation (1) includes N moisture flow rates ($\dot{m}_v$) from each source or sink i. Common sources and sinks of moisture (Figure 1a) are moisture gains or losses from ventilation (and infiltration), moisture losses from HVAC equipment, and moisture gains from internal sources (e.g., people).

Effective Moisture Penetration Depth (EMPD) Model

The EMPD model includes the same moisture sources and sinks as the EC model, but the capacitance of the room air is left unaltered and instead two material nodes are used to model the material moisture capacitance: a surface-layer node for short term fluctuations in humidity and a deep-layer node for longer term fluctuations (see Figure 1b). The node for the room air is separated from the node for the material with a mass-transfer resistance. A moisture balance on the room air gives:

$$\rho_{air}V\frac{d\omega_{room}}{dt} = \sum_{i=1}^{N}\dot{m}_{v,\,i} - \sum_{j=1}^{N}\frac{\omega_{room}-\omega_{surf,\,j}}{R_{1,\,j}} \tag{2}$$

Instead of using the EC multiplier on the room air, the last term on the right-hand-side accounts for the moisture transfer between the room air and each surface j. The surfaces are given a fictitious humidity ratio, ω_{surf}, which is the humidity ratio in equilibrium with the moisture content of the surface layer. The mass transfer resistance, R_1, includes both an air-side boundary layer resistance and a diffusive resistance inside the material. As opposed to the EC model, this resistance results in delayed buffering from each surface depending on the air velocity in the room and the moisture properties of the material.

As shown in Figure 1b, the EMPD model also includes a deep layer, which provides moisture buffering for humidity fluctuations on the order of weeks or months. For many building constructions and furnishings, this deep layer is generally needed to match the finite-difference model results (see Woods et al. [2013]). Note that the computation time needed for this EMPD model, which uses two nodes, is still much smaller than the computation time needed for finite-difference models, which use more than ten nodes (a finite-difference model with only two nodes would not be as accurate as this EMPD model). Finite-difference models also generally require more iterations to completely resolve the temperature and humidity profile in the wall.

Additional equations are needed to solve for the moisture content of the surface layer and deep layer nodes:

$$\begin{aligned}&\rho_{matl}Ad_{EMPD}\left.\frac{du}{d\phi}\right)_j\frac{1}{\omega_{sat}}\frac{d\omega_{surf,\,j}}{dt}\\&=\frac{\omega_{room}-\omega_{surf,\,j}}{R_{1,\,j}}-\frac{\omega_{surf,\,j}-\omega_{deep,\,j}}{R_{2,\,j}}\end{aligned} \tag{3}$$

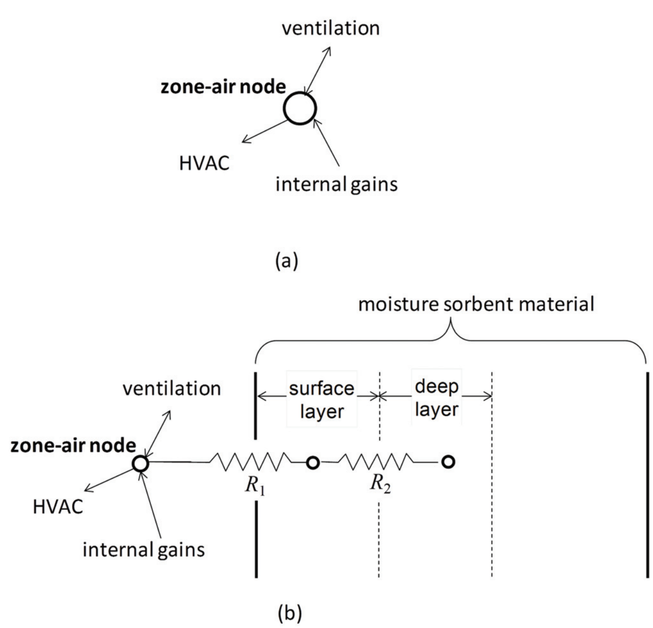

Figure 1 *Summary of transport resistances and capacity nodes for (a) effective capacitance model and (b) effective moisture penetration depth model.*

$$\left(\rho_{matl} A d_{EMPD-deep} \frac{du}{d\phi}\right)_j \frac{1}{\omega_{sat}} \frac{d\omega_{deep,\,j}}{dt} = \frac{\omega_{surf,\,j} - \omega_{deep,\,j}}{R_{2,\,j}} \tag{4}$$

where ρ_{matl} is the dry density of the material, u the moisture content of the material (kg/kg), $du/d\phi$ the slope of the moisture sorption curve, and $d_{EMPD\text{-}deep}$ and d_{EMPD} the effective penetration depths for the deep and surface layers, respectively. The transport resistances (R_1 and R_2) include the convective mass transfer resistance of the boundary layer and diffusive resistances of the material. These can be calculated with the equations in Woods et al. (2013).

Estimating the Models' Parameters

The EC and EMPD models use different parameters to represent the moisture buffering of materials. There is only one parameter for the EC model: the effective capacitance. In this study, we use values of 5, 15, 30, and 45. This extends beyond the range of 10 to 25 suggested previously (EPA 2001). We also simulate a home with no material moisture buffering (EC = 1).

In the EMPD model, there are six parameters for each buffering material: the surface area, moisture sorption curve, density, permeability, and two penetration depths (d_{EMPD} and $d_{EMPD\text{-}deep}$). While not explicitly required in the model, we also include a coating permeance for the paint on the gypsum walls and ceilings.

The simulated house includes the following moisture buffering materials:

- Painted gypsum on the interior surface of exterior walls and on partition walls
- Painted gypsum on ceilings
- Carpet flooring
- Soft (cotton) and hard (finished wood) furniture

The density and permeability of these materials are assumed constant and are listed in Table 2, while the moisture sorption slopes ($du/d\phi$) are functions of the RH, as shown in Figure 1. The penetration depths for the surface and deep layers are calculated based on these material properties, as discussed in Woods et al. (2013).

Calculating the penetration depths also requires an assumption for the short-term and long-term cycle times for the humidity fluctuations, which coincide with the latent loads on the building. These penetration depths are calculated with:

$$d_{EMPD} = \sqrt{\frac{\delta_{derm}\, p_{sat}\, \tau}{\rho_{mail} \dfrac{du}{d\phi}\, \pi}} \tag{5}$$

where δ_{perm} is the vapor permeability, p_{sat} the saturation vapor pressure, and τ the humidity cycle period. This study uses τ = 24 hours for d_{EMPD}, which buffers high-frequency loads such as internal gains, and τ = 10 days for $d_{EMPD\text{-}deep}$, which buffers low-frequency loads such as changes in the ventilation load due to the weather. Woods et al. (2013) used a thick block of concrete for their test case, which resulted in penetration depths that were always less than the material thickness. In this study, $d_{EMPD\text{-}deep}$ for the soft furnishings and the carpet is on the order of 100 mm and 35 mm, respectively, which would normally be thicker than the actual material thickness. It is unclear exactly how to address this issue. There are generally additional materials under the carpet, and possibly under or behind the soft furnishings. In this study, we adjusted the penetration depths so that they were on the same order of magnitude as the material thickness.

Unlike the EC model, the EMPD model requires inputs for the surface area of each moisture-buffering material. The wall and ceiling surface areas were based on the geometry of the house. We estimated material surface areas for the carpet and hard and soft furnishings using engineering judgment for typical furnishings in a three bedroom, 223 m^2 (2400 ft^2) house. These represented the medium buffering level shown in Table 3. The low and high buffering levels were scaled from the medium values to bound realistic furnishing levels.

While these two models are fundamentally different, we can compare a rough estimate of the overall moisture capacitance of the EMPD model with the EC values from above. Consider the surface areas for the medium buffering

Table 2. EMPD Moisture Properties

Material	Density, kg/m^3 (lb/ft^3)	Permeability, kg/m·s·Pa (gr/ft·h·in. Hg)	Coating Permeance, ng/s·m^2·Pa (perms)	d_{EMPD}, mm (in.)	$d_{EMPD\text{-}deep}$, mm (in.)
Carpet	220[a] (14.2)	3E-11[a] (1.72)	n/a	11.1 (0.44)	16.8 (0.66)
Gypsum	800[a] (51.6)	2E-11[a] (1.14)	570[d] (10)	5.8 (0.23)	18.1 (0.71)
Wood furniture	512[a] (33)	2E-12[a] (0.114)	n/a	1.3 (0.05)	4.0 (0.157)
Soft furniture	250[b] (16.1)	5E-10[c] (28.6)	n/a	12.7 (0.5)	0.0 (0.0)

[a] Kumaran 1996
[b] Svennberg 2005
[c] Kniest et al. 1998
[d] Walls and ceilings are assumed to be painted with a 10-perm paint

level, the surface penetration depths, and the material densities. These allow us to calculate an effective mass of each material:

$$\textit{Effective Mass} = \rho_{matl} A d_{EMPD} \tag{6}$$

Combining these with an average moisture sorption curve from Figure 2, we can calculate the mass of moisture that will be absorbed by each material for a given range in RH ($\Delta\phi$):

$$\textit{Moisture Absorbed} = (\textit{Effective Mass})\Delta\phi\frac{du}{d\phi} \tag{7}$$

Assuming an air temperature of the space, we can convert the $\Delta\phi$ into a difference in humidity ratio ($\Delta\omega$), which leads to an effective air mass:

$$\textit{Effective Air Mass} = \frac{\textit{Moisture Absorbed}}{\Delta\omega} \tag{8}$$

If we use a range in rh of 40% to 60%, the effective air mass of the EMPD surface layers for the medium buffering case is around 9600 kg (21,160 lbs), which is around EC = 16. Including the deep layers increases this to EC = 38. Keep in mind, though, that the models are inherently different, and this conversion is just an approximation.

RESULTS AND DISCUSSION

The simulations described above are used to assess the appropriateness of the EC and EMPD models for use in whole-building simulations. The importance of differences between the two models depends on the goal of the simulation. The sections below consider the accuracy of RH predictions, energy use predictions, and the effects of moisture buffering on equipment selection.

Predicting Relative Humidity

High-frequency humidity loads are difficult to dampen because of the slow rate of transfer into sorptive materials. This is captured in the EMPD model with the transport resistance between the room air and the material surface layer. It uses actual permeabilities for the sorptive materials and their low-perm coatings, as well as the air-side resistance to moisture transfer. As noted previously, the EC model does not include a resistance between the room air capacitance and the capacitance of the materials, and this generally means the EC model will miscalculate the dynamics of high-frequency loads.

The two-layer EMPD model gives more realistic responses to lower frequency humidity loads. The EC model cannot dampen longer term humidity loads without also affecting the response to high frequency humidity loads. This is a key difference between the EMPD and EC models. They give different responses to humidity loads of different frequencies.

This is illustrated in Figure 3, which shows the annual RH traces for the high-buffering EMPD case and for effective capacitance values of 5 and 45. The figures show the results for both Houston (left) and Orlando (right). The key drawback of the EC model is that it cannot predict the response to all moisture loads correctly, regardless of the EC value chosen.

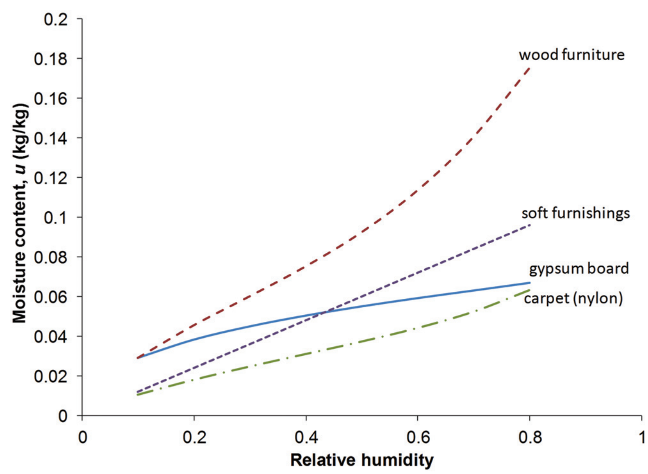

Figure 2 *Moisture sorption curves of materials. Wood furniture, gypsum board, and carpet are from Kerestecioglu et al. 1988 while soft furnishings is cotton sorption curve from Svennberg 2005.*

Table 3. Humidity Buffering Surface Areas (for EMPD Simulations)

	Moisture Buffering Level		
	Low	**Medium**	**High**
Carpet surface area, m^2 (ft^2)	67 (721)	145 (1,61)	212 (2282)
Soft furniture, m^2 (ft^2)	25 (269)	75 (807)	200 (2153)
Wood furniture, m^2 (ft^2)	25 (215)	60 (646)	150 (1615)
Painted gypsum (interior walls), m^2 (ft^2)	223 (2400)	223 (2,400)	223 (2,400)
Painted gypsum (exterior walls), m^2 (ft^2)	175 (1,80)	175 (1,880)	175 (1,880)
Painted gypsum (ceiling), m^2 (ft^2)	223 (2400)	223 (2400)	223 (2400)

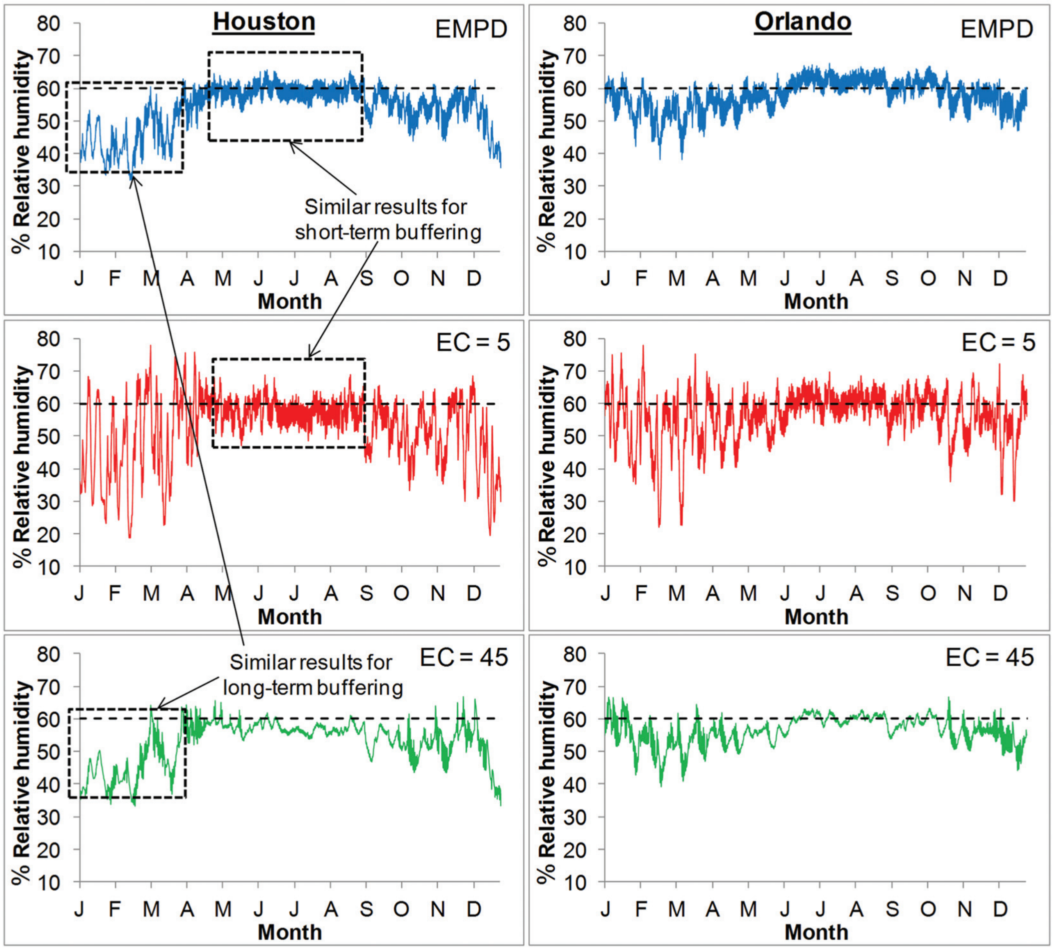

Figure 3 *Zone relative humidity for Houston (left) and Orlando (right). Top plot is the high-buffering EMPD case, while bottom two plots are the EC model at two different values for the effective capacitance.*

Figure 3 shows that the EC = 5 case generally predicts the correct response to the high-frequency humidity loads due to air conditioner moisture removal (summer), but it does not provide enough damping to the low-frequency humidity loads due to changes in the weather (winter and swing seasons). Alternatively, using EC = 45 generally matches the low frequency loads, but overdamps the high-frequency loads.

Figures 4 and 5 show more clearly the RH fluctuations for two months: February and August. The February results in Figure 4 illustrate a case with low-frequency humidity loads. The EC = 45 case resembles the EMPD response, which buffers these low frequency loads. Using EC = 5 provides little buffering for these low frequency fluctuations, resulting in large swings in the humidity not seen in the EMPD case. The August results (Figure 5), where the air conditioner is running intermittently to meet the sensible load, illustrate a case with high frequency humidity loads. The EC = 5 case resembles the EMPD response, providing buffering for high-frequency loads, while using EC = 45 provides too much buffering.

These results show that if the goal of the simulations is to predict the indoor RH throughout the year, the EC model will likely predict results much different from the EMPD model. If the goal is instead to predict high RH events to estimate the risk of moisture-related issues in the building, these differences may be less important. There will certainly still be differences, such as in Houston in August (Figure 5), where the EC = 45 case predicts much fewer hours above 60% rh than the EMPD or EC = 5 results. But what do these results tell us about the need for dehumidification or the risk of having moisture-related problems, such as mold growth?

While some guidelines (ASHRAE 2013) exist to indicate high probability of moisture problems, these guidelines refer to a maximum surface RH, as opposed to an average indoor RH. Since the EC model does not calculate surface conditions, we instead use the *indoor* RH metrics in Table 4 as surrogates, which have been used previously (Rudd and Henderson 2007; Fang et al. 2011; Winkler et al. 2013).

These data show some similarities. In both the EMPD and EC cases, the hours above 60% rh and the number of

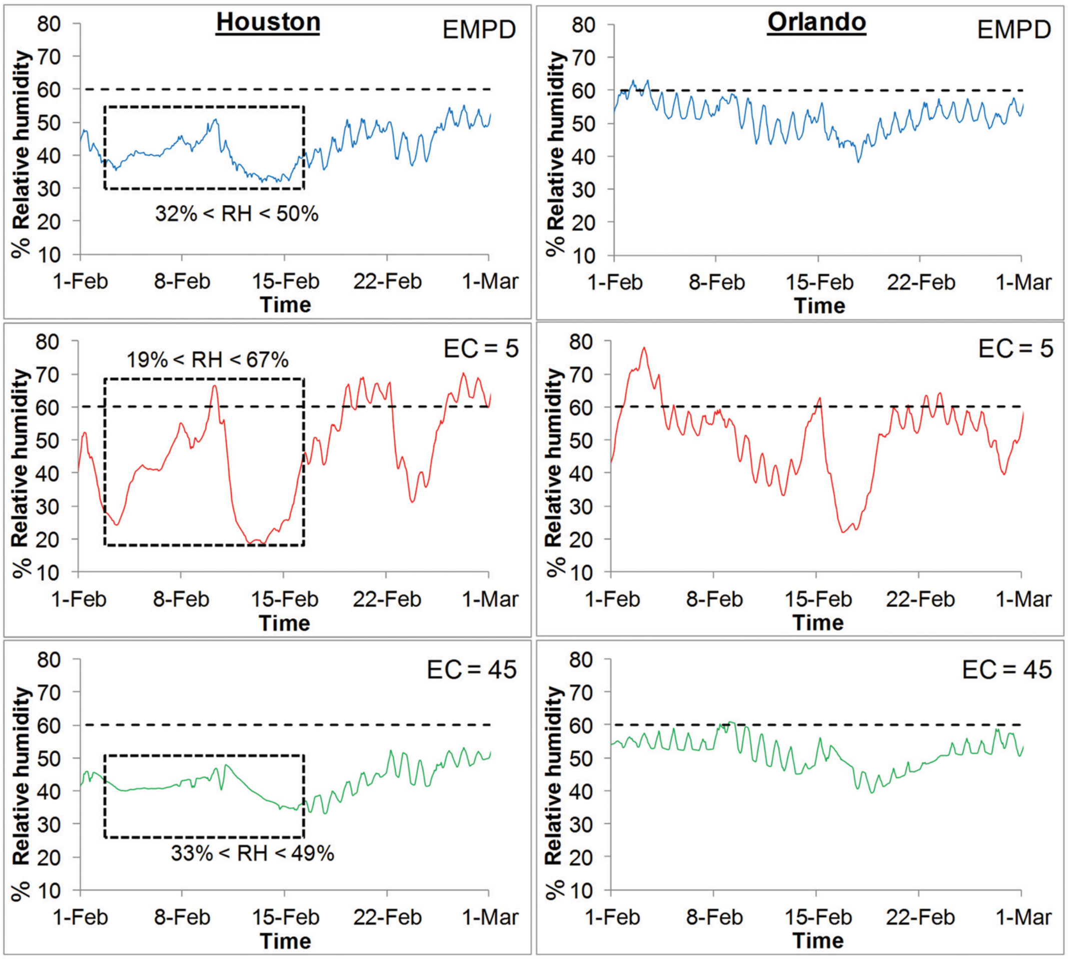

Figure 4 *Close-up view of February from Figure 3.*

excursions longer than 4 hours are high enough to warrant supplemental dehumidification. Both models also show similar trends: higher levels of buffering decrease the hours above 60% rh and decrease the number of excursions.

There are also some important differences. The hours above 60% rh and the number of excursions for the EMPD cases are higher than those for the EC cases. The EMPD model generally predicts many short excursions, compared to fewer, but longer, excursions predicted by the EC model. The resistance between the indoor air node and the material node (Figure 1b) slows the buffering in the EMPD model, which results in more short-term 'spikes' in humidity. On the other hand, an excursion may last several days or weeks in the EC model because of the small amplitude of the daily RH fluctuations (see, e.g., the EC = 45 case for Orlando in Figure 5). The lower amplitude of the RH profile means there are fewer times where the RH cycles back and forth between an RH greater than 60% and an RH less than 60%.

Since we have results for two cities, we can make a preliminary evaluation about consistency between the two models. If we interpolate between the different EC cases for Houston, EC = 10 and EC = 25 give about the same hours above 60% rh as EMPD low and EMPD high. In Orlando, EMPD low and EMPD high are about the same as EC < 5 and EC = 10. This indicates that converting between the two models is inconsistent across climates. This is due to the inherent differences in the models; the two models cannot be made equivalent.

However, if someone is interested in understanding the risks of moisture-related problems, the two models may lead to the same conclusions. Based on the results presented here, it appears that EC values of around 10 to 15 (which are commonly used) will lead to similar overall conclusions (e.g., there is or is not a risk of mold growth) as the EMPD model, particularly if hours above 60% is the relevant metric. This is true for the two cities and homes analyzed here, but may not hold universally. It depends on what parameters are selected for each model. As discussed in the Methods section, the EMPD model includes more realistic inputs, which can presumably give more reliable results if these material properties are known or can be measured. Future research will focus on these two areas: (1) generalizing this study to different buildings and different climates and (2) developing methods to measure the EMPD properties in-situ in a home.

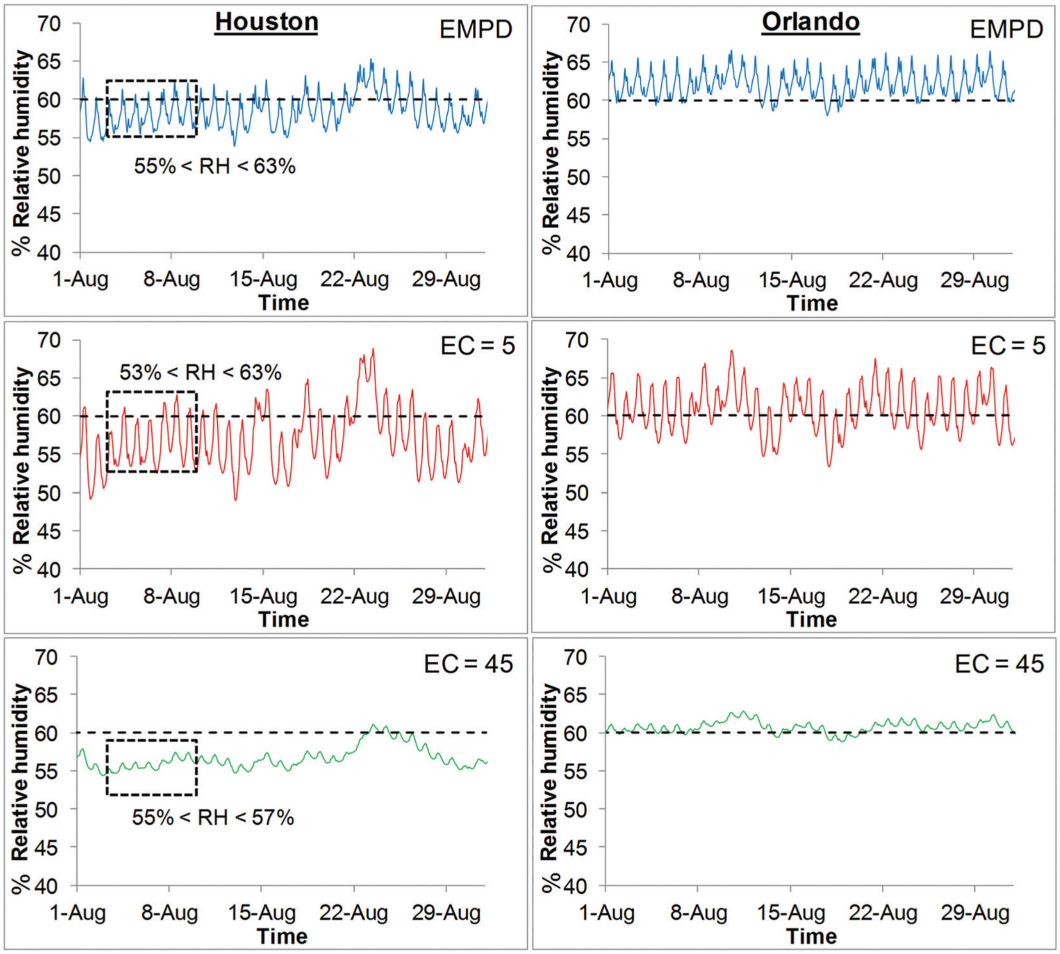

Figure 5 *Close-up view of August from Figure 3.*

Table 4. Indoor RH Metrics for the EMPD and EC Models for a Range of Moisture Capacitance Levels

		No Buffering	EMPD			Effective Capacitance			
			Low	Medium	High	EC = 5	EC = 15	EC = 30	EC = 45
Houston	Total Number of Hours with RH > 60%	2704	1598	1182	754	1,995	1084	670	494
	Number of Excursions [a]	265	206	196	166	166	78	54	49
	Average Excursion Length (h)	10.2	7.8	6	4.5	12.0	13.9	12.4	10.1
	Maximum Excursion Length (h)	83	43	43	41	85.5	83	64.3	61
	Number of Excursions > 4 h	216	155	106	45	124	44	33	29
	Number of Excursions > 8 h	140	68	43	22	71	29	26	19
Orlando	Total Number of Hours with RH > 60%	3266	2936	2755	2515	2,805	2356	2,055	1,993
	Number of Excursions	345	273	250	209	210	129	88	75
	Average Excursion Length (h)	9.5	10.8	11	12	13.4	18.3	23.4	26.6
	Maximum Excursion Length (h)	66	93	111	134	90.5	131	258	400
	Number of Excursions > 4 h	257	181	156	107	155	88	56	45
	Number of Excursions > 8 h	199	131	115	75	118	72	44	36

[a] An "excursion" is defined as a unique event when indoor RH exceeds 60%.

Predicting Energy Use

Differences between the two models can also impact the predicted energy use for air conditioners and dehumidifiers, which is important if a researcher wants to understand the energy use related to temperature and humidity control. Figures 6 and 7 show the required cooling energy for Houston and Orlando, respectively. Three cases are shown: uncontrolled humidity (no dehumidifier), humidity controlled to 60% rh, and humidity controlled to 55% rh.

For the case with no humidity control, the cases with moisture buffering predict slightly higher energy use than the case with no buffering. This is because the RH at the evaporator coil inlet for these cases is slightly higher. Figure 8 shows a histogram of the RH while the air conditioner is running. The air conditioner provides a certain level of sensible cooling to this air to meet the temperature setpoint, but since the humidity is higher for the EMPD and EC cases, the air conditioner simultaneously provides more latent cooling. Thus, it provides more total cooling, and uses slightly more energy, to maintain the same temperature setpoint.

In Figures 6 and 7, the second and third columns show the energy use when the RH is controlled to 60% and 55%, respectively. Since the temperature setpoints have not changed, the energy use is higher when controlling humidity. In general, the energy use predicted by the EC model is lower than that predicted by the EMPD model. If we compare the commonly used value of EC = 15 and the EMPD medium case, the EC model predicts 24% less dehumidification energy (4% less total cooling energy) in Houston and 35% less dehumidification energy (17% less total cooling energy) in Orlando. Note that the trend from EMPD low to EMPD high also differs from the trend from EC = 5 to EC = 45, particularly for the cases in Orlando.

These differences can be seen more easily by using the no-buffering case as a benchmark for comparison. Table 5 shows relative differences in energy use compared to the no-buffering case. The trends with moisture buffering level correlate reasonably well with the hours above 60% rh when humidity is uncontrolled (Table 4). For example, adding moisture buffering to a home in Orlando has a smaller effect on energy use than it does in Houston, which is consistent with the effect of buffering level on hours above 60% rh.

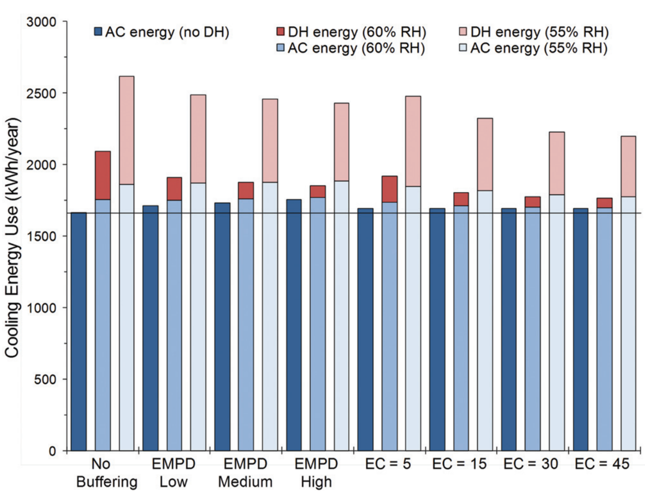

Figure 6 *Energy use for air conditioner (AC) and dehumidifier (DH) in Houston with different levels of moisture buffering. The cases with humidity control use a 45 pints/day (21.3 L/day) dehumidifier with an efficiency of 1.5 L/kWh. Humidistat setpoint for each simulation is indicated in parentheses.*

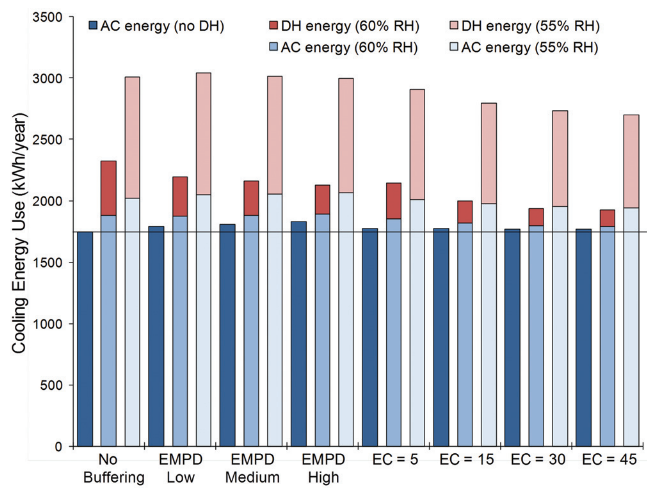

Figure 7 *Energy use for air conditioner (AC) and dehumidifier (DH) in Orlando with different levels of moisture buffering. The cases with humidity control use a 45 pints/day (21.3 L/day) dehumidifier with an efficiency of 1.5 L/kWh. Humidistat setpoint for each simulation is indicated in parentheses.*

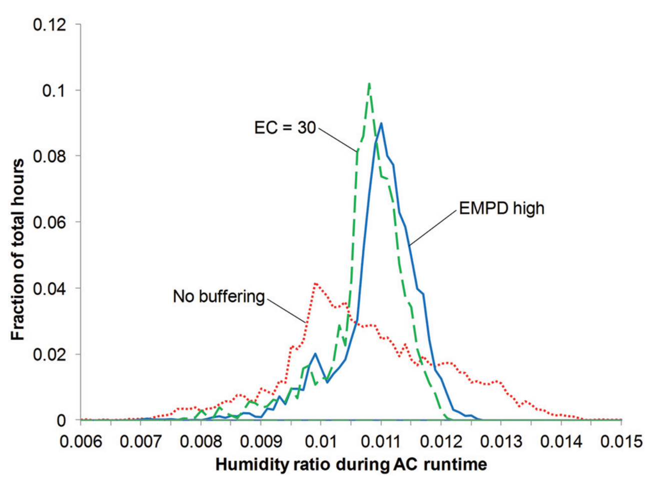

Figure 8 *Indoor humidity ratio frequency distribution for Houston while air conditioner is on. No dehumidification.*

Table 5. Energy Use Relative to No-Buffering Case

		60% rh Control		55% rh Control	
		Total Cooling Energy	DH Energy	Total Cooling Energy	DH Energy
Houston	EMPD Low	–9%	–54%	–5%	–18%
	EMPD Medium	–10%	–65%	–6%	–23%
	EMPD High	–11%	–75%	–7%	–28%
	EC = 5	–8%	–45%	–5%	–16%
	EC = 15	–14%	–73%	–11%	–33%
	EC = 30	–15%	–78%	–15%	–42%
	EC = 45	–16%	–80%	–16%	–44%
Orlando	EMPD Low	–6%	–28%	1%	0%
	EMPD Medium	–7%	–37%	0%	–3%
	EMPD High	–8%	–47%	0%	–6%
	EC = 5	–8%	–34%	–3%	–9%
	EC = 15	–14%	–59%	–7%	–17%
	EC = 30	–17%	–68%	–9%	–21%
	EC = 45	–17%	–70%	–10%	–23%

Similar to the results above, the difference between EMPD low and EMPD high do not coincide with EC = 5 and EC = 45, respectively, and the results are not consistent from one city to the other. The EMPD model results fall between EC = 5 and EC = 15 in Houston, while in Orlando they seem to agree for EC < 5 and EC = 10.

It is important to note that these simulations (both EMPD and EC) do not model the release or uptake of the heat of sorption when moisture is adsorbed by the materials. This effect can change the sensible heat ratio of the building and can affect the heating or cooling energy. Future research is planned to investigate this effect.

Selecting HVAC Equipment

This section discusses potential differences between the two models when selecting HVAC equipment. In particular, we look at dehumidifier sizing and the impacts of variable speed air conditioners.

Dehumidifier Sizing. The level of moisture buffering affects how large a dehumidifier will need to be to maintain the indoor RH. Figure 9 shows the dehumidifier size for different levels of buffering to limit the time spent above 60% rh to 100 hours and 400 hours. The solid lines are the dehumidifier sizes for EC levels from 1 to 45. The shaded bands correspond to the range of dehumidifier sizes for EMPD low to EMPD high. The dotted, horizontal line inside the band is the EMPD medium case, while the top and bottom dashed lines are for EMPD low and high, respectively. The figures indicate that dehumidifier size decreases with increased buffering for the EMPD model. This is true for the EC model initially, but not for higher levels of buffering.

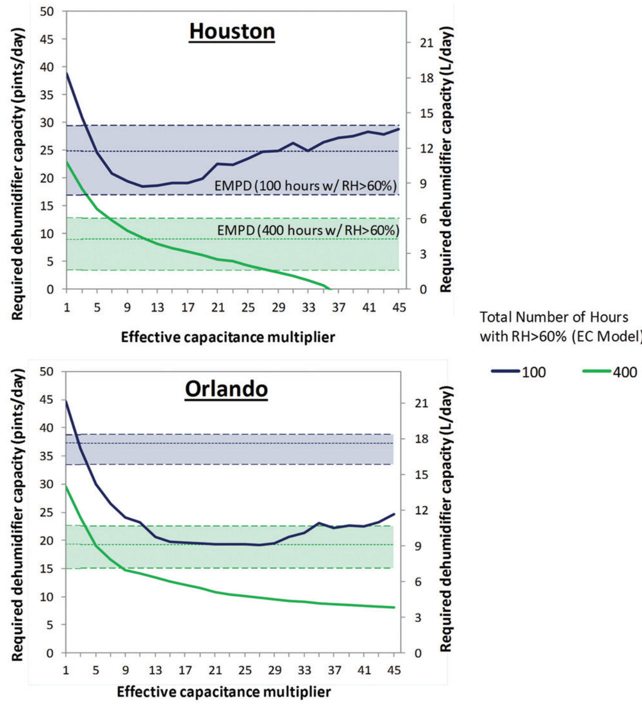

Figure 9 *Required dehumidifier size as a function of the level of moisture buffering. The EMPD band includes lines for the low, medium, and high buffering levels, with the low buffering line at the top.*

As an example, consider a case where a dehumidifier is sized to restrict the time above 60% rh to 100 hours per year. In both Houston and Orlando, using EC = 15 leads to a dehumidifier of approximately 9.5 L/day (20 pints/day). For EMPD medium, the required dehumidifier size is 11.8 L/day (25 pints/day) in Houston, but 17.5 L/day (37 pints/day) in Orlando. This is 300 to 500 W (1000 to 1700 Btu/h) of latent cooling capacity, which is on the order of 5% of the total cooling capacity of the air conditioner required for this low-load home.

Comparing the EMPD and EC results, we see that the estimated dehumidifier size may be different between the two models. The results also indicate inconsistencies between the two cities, similar to the RH statistics in Table 4. However, in the cases illustrated here, a modestly sized dehumidifier

(40 pints/day) will provide adequate dehumidification in both cities regardless of the level of moisture buffering.

Air Conditioners with Variable Speed Compressors. In a previous study, Winkler et al. (2013) used the EMPD model to look at variable speed air conditioners. They concluded that these air conditioners do not effectively manage latent loads during much of the year, with roughly 4500 hours above 60% rh in Houston and 5900 hours above 60% rh in Orlando. In this study, we ran the same analysis with the EC model, which confirmed that these conclusions will be the same regardless of the chosen moisture model. The RH for these simulations, whether performed with the EMPD or EC models, are higher than 60% throughout most of the year, and the fluctuations around the mean RH are less important when looking at hours above 60%.

CONCLUSIONS

This study used whole-building simulations of homes in hot-humid climates to compare the EC and EMPD moisture models. The variation of RH throughout the year was significantly different between these two models. This is due to the added transport resistances in the EMPD model, both between the zone air and the surface layer and between the surface layer and the deep layer. The second resistance enables the use of a deep layer to account for buffering of humidity loads of lower frequencies (on the order of weeks). The EC model is incapable of buffering these loads of different frequencies. The EC = 45 case matches the EMPD model for low-frequency loads, but overdamps high-frequency loads. The EC = 5 case matches the EMPD model for high-frequency loads, but underdamps low-frequency loads.

Regarding the simple moisture-risk metrics, the EMPD model predicts many short excursions above 60% rh, while the EC model predicts fewer excursions of longer duration. This is because the transport resistances in the EMPD model slow the buffering, resulting in more short-term spikes in humidity. However, if hours above 60% rh is used as a metric, the EMPD and EC models generally predict similar results, except for high EC values (EC > 30). Comparing the results from Houston and Orlando showed that a simulation using a certain value of EC in one city can agree with the EMPD results, but that the same EC value in the other city may not agree with the EMPD results.

The two moisture modeling strategies predict different cooling energy use. When humidity is uncontrolled, the buffering has a small effect, but when humidity is controlled, higher buffering generally results in lower energy use. The EMPD model predicted slightly larger air conditioner and dehumidifier energy use than most of the EC cases.

So which model should be used? Comparing each model's assumptions, the EMPD model is certainly more realistic. And this study showed that the simplifying assumptions in the EC model can lead to unrealistic results. But this question cannot be fully answered by this paper, and we hesitate to recommend one model over the other without further research and some experimental data.

The lack of experimental data is one limitation to this study. The moisture properties of the materials for the EMPD model were taken from material databases and the surface areas of the different materials were estimated based on engineering judgment. Future research will use an experimental method to measure, in-situ, the moisture properties of the materials in a home, and will also infer the surface areas of the materials.

A second limitation is that both the EMPD and EC models used in this study were isothermal. A next step in this research is to change the EMPD model to a non-isothermal model. This means the model will include the effects of the latent heat that is absorbed or released at the material surface due to water vapor sorption and desorption. It will also model the changing temperature at the wall surface due to this latent heat transfer. We plan to implement this updated model into the EnergyPlus software.

ACKNOWLEDGMENTS

This work was supported by the U.S. Department of Energy under Contract No. DE-AC36-08-GO28308 with the National Renewable Energy Laboratory.

NOMENCLATURE

A	=	surface area (m^2)
d_{EMPD}	=	effective moisture penetration depth (m)
EC	=	effective moisture capacitance (m^3/m^3)
m_v	=	water vapor flow rate (kg/s)
p_{sat}	=	saturation vapor pressure
R	=	mass transfer resistance (s/kg)
RH	=	relative humidity
t	=	time (s)
u	=	moisture content of material (kg/kg)
V	=	volume (m^3)
δ_{perm}	=	vapor permeability (kg/m·s·Pa)
ρ	=	density (kg/m^3)
ϕ	=	relative humidity
τ	=	cycle period used in penetration depth calculation (s)
ω	=	humidity ratio (kg/kg)

Subscripts

air	=	property of indoor air
deep	=	material deep layer
i	=	index of moisture flows
j	=	index of surfaces
matl	=	property of material
sat	=	saturated
surf	=	material surface layer

REFERENCES

Abadie, M.O. and K.C. Mendonca, 2009. Moisture performance of building materials: From material characterization to building simulation using the Moisture Buffer Value concept, *Build. Environ*. 44, 388-401.

Antretter, F., F. Sauer, T. Schoepfer, A. Holm. Validation of a hygrothermal whole building simulation software, in *Proceedings of Building Simulation 2011*: 12th Conference of International Building Performance Simulation Association. Sydney, 2011.

ASHRAE, 2004. ANSI/ASHRAE Standard 62.2-2004, *Ventilation and Acceptable Indoor Air Quality in Low-Rise Residential Buildings*. Atlanta: ASHARE.

ASHRAE, 2012. ASHRAE Position Document on Limiting Indoor Mold and Dampness in Buildings. Atlanta: ASHARE.

Bornehag, C.G., J. Sundell, T. Sigsgaard, 2004. Dampness in buildings and health (DBH): Report from an ongoing epidemiological investigation on the association between indoor environmental factors and health effects among children in Sweden, *Indoor Air*. 14, 59-66.

Cunningham, M.J., 1988. The moisture performance of framed structures—a mathematical model, *Build. Environ*. 23, 123-35.

Cunningham, M.J., 1992. Effective penetration depth and effective resistance in moisture transfer, *Build. Environ*. 27, 379-86.

DOE, 2012. EnergyPlus Engineering Reference, US Department of Energy.

EPA, 2001. Indoor Assessment Tool (IHAT) reference manual. US Environmental Protection Agency.

Fang, L., G. Clausen, P.O. Fanger, 1998. Impact of temperature and humidity on the perception of indoor air quality, *Indoor Air-International Journal of Indoor Air Quality and Climate*. 8, 80-90.

Fang, X., J. Winkler, D. Christensen, Using EnergyPlus to perform dehumidification analysis on Building America homes, *HVAC&R Res*. 17 (2011) 268-83.

Haverinen, U., M. Vahteristo, D. Moschandreas, A. Nevalainen, T. Husman, J. Pekkanen, 2003. Knowledge-based and statistically modeled relationships between residential moisture damage and occupant reported health symptoms, *Atmospheric Environment*. 37, 577-85.

Henderson, H., D. Shirey, C.K. Rice, 2008. Can conventional cooling equipment meet dehumidification needs for houses in humid climates?, in 2008 ACEEE Summer Study on Energy Efficiency in Buildings. Pacific Grove, CA.

Hendron, R. and C. Engebrecht, 2010. Building America House Simulation Protocols. National Renewable Energy Laboratory, TP-5500-49246.

ICC, 2009. International Code Council, *International Energy Conservation Code*.

James, C., C.J. Simonson, P. Talukdar, S. Roels, 2010. Numerical and experimental data set for benchmarking hygroscopic buffering models, *Int. J. Heat Mass Tran*. 53, 3638-54.

Janssen, H. and S. Roels, 2009. Qualitative and quantitative assessment of interior moisture buffering by enclosures, *Energ. Buildings*. 41, 382-94.

Kerestecioglu, A., M. Swami, R. Dabir, N. Razzaq, P. Fairey, 1988. Theoretical and Computational Investigation of Algorithms for Simultaneous Heat and Moisture Transport in Buildings. Florida Solar Energy Center, DOE/SF/16305-2.

Kerestecioglu, A., M. Swami, A. Kamel, 1990. Theoretical and computational investigation of simultaneous heat and moisture transfer in buildings: “Effective penetration depth” theory, *ASHRAE Transactions*. 96, 447-54.

Kniest, F.M., K.-U. Blank, N. Kalsdorf, 1998. Differences between air permeable and air-nonpermeable fabrics on the efficacy and comfort of mite and allergen-proof encasings, *Journal of Aerosol Science*. 29, Supplement 1, S1285-S86.

Kumaran, M.K., 1996. Final Report Task 3 Hygrothermal properties of building materials. Annex 24: Heat Air and Moisture Transfer in Insulated Envelope Parts, IEA.

Künzel, 1995. Simultaneous heat and moisture transport in building components. PhD thesis, Fraunhofer Institute of Building Physics Fraunhofer IRB.

Künzel, H.M., A. Karagiozis, and A. Holm. 2001. A hygrothermal design tool for architects and engineers, Chapter 9. In *ASTM Manual 40: Moisture Analysis and Condensation Control in Buildings Envelopes*. H.R. Treschsel, ed. West Conshohocken, PA: ASTM International.

Künzel, H.M., A. Holm, D. Zirkelbach, A.N. Karagiozis, 2005. Simulation of indoor temperature and humidity conditions including hygrothermal interactions with the building envelope, *Sol. Energy*. 78, 554-61.

Lstiburek, J., 2009a. Building Science Insights - Thermodynamics: It's Not Rocket Science. Building Science Corporation, Report BSI-02. Available at: http://www.buildingscience.com/documents/insights/bsi-021-thermodynamics-its-not-rocket-science/files/bsi-021_thermodynamics_rocket_science.pdf.

Lstiburek, J., 2009b. Building Science Digests – Moisture Control for New Residential Buildings. Report BSD-012. Available at: http://www.buildingscience.com/documents/digests/bsd-012-moisture-control-for-new-residential-buildings/files/bsd-012_moisture_control_new_bldgs.pdf.

Plagge, R., G. Scheffler, A. Nicolai, 2007. Experimental Methods to Derive Hygrothermal Material Functions for Numerical Simulation Tools, in Thermal Performance of the Exterior Envelopes of Whole Buildings X International Conference. Clearwater Beach, FL.

PNNL & ORNL, 2010. Guide to Determining Climate Regions by County, Pacific Northwest National Laboratory, PNNL-17211.

Rode, C. and K. Grau, 2008. Moisture buffering and its consequence in whole building hygrothermal modeling, *Journal of Building Physics*. 31, 333-60.

Rudd, A. and H. Henderson, 2007. Monitored indoor moisture and temperature conditions in humid-climate US residences, *ASHRAE Transactions*. 113, 435-49.

Steeman HJ, Van Belleghem M, Janssens A, De Paepe M. 2009. Coupled simulation of heat and moisture transport in air and porous materials for the assessment of moisture related damage. *Build. and Environ*. 44(10): 2176-84.

Steeman, M., A. Janssens, H.J. Steeman, M. Van Belleghem, M. De Paepe, 2010. On coupling 1D non-isothermal heat and mass transfer in porous materials with a multizone building energy simulation model, *Build. Environ*. 45, 865-77.

Svennberg, K., 2005. Sorption isotherms for textile fabrics and foam used in the indoor environment, Report TVBH-7227, Lund Institute of Technology. Presented at IEA Annex 41 Meeting.

Tariku, F., K. Kumaran, P. Fazio, 2011. Determination of indoor humidity profile using a whole-building hygrothermal model, *Building Simulation*. 4, 61-78.

Walker, I.S. and M.H. Sherman, 2007. Humidity Implications for Meeting Residential Ventilation Requirements. Lawrence Berkeley National Laboratory, LBNL-62182.

Winkler, J., J. Woods, D. Christensen, 2013. Equipment and operational settings for high performance homes in hot-humid climates. National Renewable Energy Laboratory, (in review) TP-5500-57440.

Woods, J., J. Winkler, D. Christensen, 2013. Evaluation of the effective moisture penetration depth (EMPD) model for estimating moisture buffering in buildings. National Renewable Energy Laboratory, TP-5500-57441.